Heterocrystalline Structures: New Types of Superlattices?

Friedhelm Bechstedt and Peter Käckell
Friedrich-Schiller-Universität, Institut für Festkörpertheorie und Theoretische Optik, Max-Wien-Platz 1, 07743 Jena, Germany

(Received 10 March 1995)

For the first time we present results of *ab initio* calculations of the structural and electronic properties of heterocrystalline combinations of a cubic ($3C$) and a hexagonal (pH, $p = 2, 4, 6$) polytype of SiC, the material exhibiting the most pronounced polytypism. We show that these combinations give rise to a new type of "heterostructures" consisting of chemically identical but structurally different materials. For $(3C)_{N_1}(pH)_{N_2}$ superlattices we predict a similar behavior as found for type-II heterostructures.

PACS numbers: 71.25.Tn, 73.20.Dx

Polytypism is known for several semiconductors. In particular, the zinc-blende and wurtzite structures of III-V and II-VI compounds are energetically not very different, despite the rather different band structures. The group-IV compound silicon carbide (SiC) exhibits a pronounced polytypism. It crystallizes in more than a hundred different crystalline modifications, i.e., polytypes [1]. The two most extreme polytypes are zinc blende ($3C$) with pure cubic stacking of the Si-C double layers in the [111] direction and wurtzite ($2H$) with pure hexagonal stacking in the [0001] direction. The stacking of bilayers in a unit cell is commonly described by ABC for zinc blende and AB for wurtzite. The other polytypes represent combinations of these stacking sequences. For instance, two other hexagonal polytypes are $4H$ and $6H$ with repeated sequences of $ABCB$ and $ABCACB$. The electronic structures of the polytypes are rather different. Zinc-blende $3C$-SiC is characterized by the smallest indirect energy gap of 2.390 eV, whereas the hexagonal pH polytypes exhibit gaps of 3.023 eV ($p = 6$), 3.263 eV ($p = 4$), and 3.330 eV ($p = 2$) [2]. Moreover, the position of the lowest conduction-band minimum in the Brillouin zone (BZ) varies with the polytype from X (fcc BZ) to the M point ($6H$,$4H$), or the K point ($2H$) in the hexagonal BZ [3,4]. However, an ongoing debate concerns this $\mathbf{k}$-space location for $4H$ and even $6H$ (cf. Ref. [4], and references therein).

Numerous theoretical and experimental studies of semiconductor heterosystems consisting of two chemically inequivalent materials have shown drastic changes in the electronic structure in comparison with that of the underlying bulk materials. Meanwhile, crystalline SiC layers of different polytypes may be deposited by means of molecular-beam epitaxy (MBE) on different substrates and by means of different gas or solid sources [5–7]. Considering heterocrystalline layered structures of different polytypes, the fundamental question arises of how different crystal structures, or, more strictly speaking, structural symmetry changes, affect their electronic structure. As a consequence, the localization of electrons and holes in certain regions of the heterocrystalline structure has to be discussed.

In this Letter, we confirm the ideas about the electronic properties resulting for heterocrystalline structures. We examine heterocrystalline but homomaterial semiconductor systems of zinc-blende $3C$/hexagonal pH ($p = 2, 4, 6$) polytypes. As the material example, SiC is chosen because of its pronounced polytypism and the remarkable difference between the fundamental energy gaps. The resulting heterocrystalline structures do not simply represent new polytypes with averaged electronic properties and energy gaps which follow the Choyke-Hamilton-Patrick relation [3,8] with the percentage hexagonality. As a consequence of their type-II character, smaller energy gaps and different spatial localization of electrons and holes are derived.

The details of the self-consistent pseudopotential calculations in the framework of the density-functional theory (DFT) and the local-density approximation (LDA), not specified here, are like those in Refs. [3] and [9]. The geometry chosen is that of a $(3C)_{N_1}(pH)_{N_2}$ [111-0001] superlattice. A unit cell corresponds to that of an $18H$ polytype, i.e., 18 Si-C bilayers stacked in the [111] or [0001] direction, and hence contains 36 atoms. The individual bilayers fulfill the sum rule $3N_1 + pN_2 = 18$. Some results are checked for a $30H$ structure. The calculations [9,10] that include structural relaxations have shown that the different polytypes match rather perfectly in the [111-0001] direction within values smaller than 0.1%. For this reason, as a first step we replace the hexagonal lattice constants a and c by their weighted average values. The starting atomic positions are taken from the ideal polytype geometries. The atomic coordinates are optimized until the Hellmann-Feynman forces resulting in the heterocrystalline interfaces parallel to the c axis vanish. The ratio of the hexagonal lattice constants is fixed at about $c/(18a) = 0.8176$, i.e., a value very close to that found for the $6H$ polytype [9]. The single-particle wave functions are expanded in plane waves. The energy cutoff is chosen at 34 Ry because of the application of softened carbon pseudopotentials. The $\mathbf{k}$ integration is replaced by a summation over six Chadi-Cohen special points in the irreducible wedge of the BZ. The self-consistent numerical calculations are performed within DFT-LDA by means of the computer code of Stumpf and Scheffler [11].

0031-9007/95/75(11)/2180(4)$06.00

Explicitly the superlattices $(3C)_2(6H)_2$, $(3C)_2(4H)_3$, $(3C)_2(2H)_6$, and $(3C)_4(2H)_3$ are studied. The stacking patterns in the [111-0001] direction of these structures are represented in Fig. 1. The relative energetic stability of the superlattices is derived from their total energies. The energetically most favorable superlattice structure is $(3C)_2(4H)_3$. However, the energy variations are extremely small as well known from the naturally occurring polytypes [9,10]. Comparing with a zinc-blende structure, for calculating purposes represented also within the $18H$ unit cell, we find energy differences per Si-C pair of -9.0 meV $[(3C)_2(6H)_2]$, -9.8 meV $[(3C)_2(4H)_3]$, -6.6 meV $[(3C)_4(2H)_3]$, and -5.2 meV $[(3C)_2(2H)_6]$. The variation of the total energy differences with the superlattice shows a similar trend as the energy differences for the individual polytypes: There is a similar dependence on the percentage hexagonality h with a pronounced minimum at about $h = 50\%$, as in the case of naturally occurring polytypes [9]. Besides this we find a further dependence on the stacking sequences, i.e., the polytypes arranged in the superlattice cell and their repetition rate. We find the lowest energy value with -10.2 meV for the sequence $(6H)_1(4H)_3$. The increased number of atomic degrees of freedom and the interface relaxation could explain why the energies of the $18H$ structures are lower by about -7.3 meV per pair than that of $3C$ or $6H$ calculated in an $18H$ superlattice for comparison. Nevertheless, a discussion of stability should be avoided since in our calculation a static lattice is assumed and zero point vibrations—which could give contributions to the total energy of order of some meV—are not taken into account.

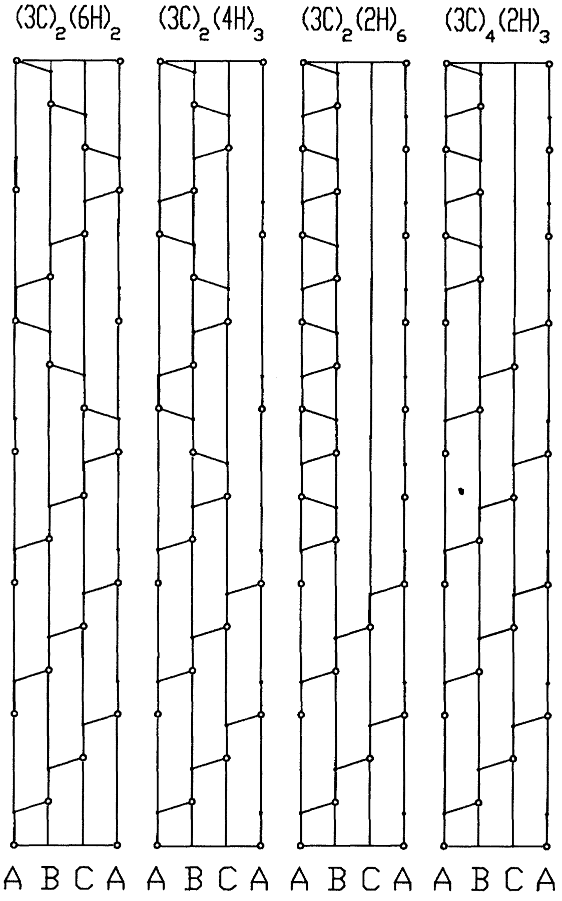

FIG. 1. Schematic representation of the $18H$ unit cells of the superlattices under consideration. The zigzag chain structures indicate the positions of Si (open circles) and C (filled circles) atoms. All atoms are located in the $(11\bar{2}0)$ plane. The different $(\bar{1}100)$ planes within the unit cells are denoted by A, B, and C to make obvious the stacking sequences.

The strongest atomic relaxations happen for the $(3C)_{N_1}(2H)_{N_2}$ structures, more strictly, in the interfaces between purely cubically and hexagonally stacked layers. On the other hand, the atomic displacements parallel to the c axis are negligible inside the material layers. Generally, the interface bonds are stretched, although the stretching is different for the two interfaces belonging to one unit cell. This effect is related to the reduced symmetry. Instead of the space group C_{6v}^4 $(P6_3mc)$ of the hexagonal polytypes only C_{3v}^1 is applicable. The actual atomic displacements depend on the stacking sequence. For the $(3C)_4(2H)_3$ and $(3C)_2(2H)_6$ superlattices the two Si-C bonds around the interface $3C \rightarrow 2H$ (cf. upper part of Fig. 1) possess lengths increased by 0.01–0.02 Å. Thereby the stretching tendency is stronger for the heterostructures with more hexagonal bilayers. On the other hand, the bonds in the interface $2H \rightarrow 3C$ (cf. lower part of Fig. 1) remain almost unchanged due to the continuation of the Si-C bond chains within the lateral extent of the unit cell. Qualitatively, the same interface effects are observed for the other structures. However, they are weaker.

The results of the DFT-LDA band-structure calculations are represented in Fig. 2, where we show the positions of the valence-band maximum at Γ and of the conduction-band minima at M and K for the described structures. The location of the band extrema may be understood in terms of the underlying bulk band structures. The valence-band maximum in all polytypes is located at the Γ point. The lowest conduction-band minimum occurs in the $6H$ and $4H$ structures at the M point. The same happens when the $3C$ band structure is represented within the BZ of a $3H$ structure [3,4]. Only in the wurtzite $2H$ case does the conduction-band minimum appear at K. The lowest conduction-band minima in $6H$, $4H$, and $2H$ are about 1 eV higher in energy than that in $3C$ [3,4]. Consequently, the M minima of the superlattices should mainly arise from that of the cubic polytype. In the artificial $3H$ structure it is located at the M point. The folding into the BZ of the $18H$ structure, however, reproduces the M point again. On the other hand, the bands between M and L are extremely flat due to the multiple folding. An additional

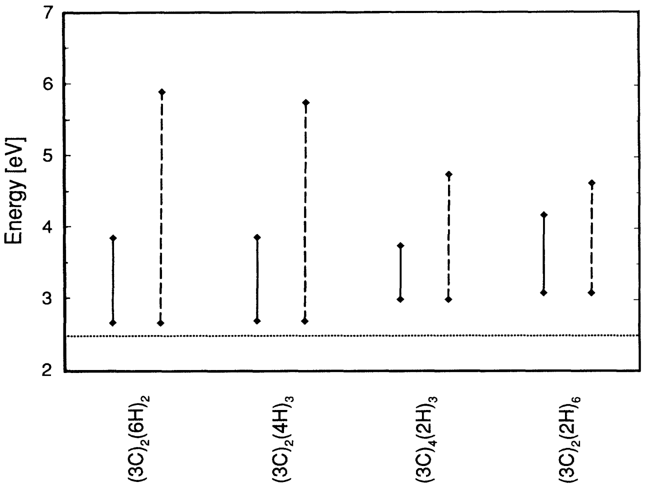

FIG. 2. Positions of the valence-band maximum at Γ (lower diamonds) and of the conduction-band minima at M and K (upper diamonds) from DFT-LDA band-structure calculations. The solid (dashed) lines denote the indirect energy gaps $\Gamma \rightarrow M$ ($\Gamma \rightarrow K$). The energy zero is identified with the tails of the atomic pseudopotentials. For comparison the position of the valence-band maximum of pure $3C$-SiC is indicated by a horizontal, dotted line.

pronounced minimum at K is observed for the $(3C)_2(2H)_6$ and $(3C)_4(2H)_3$ superlattices. It represents the remarkable wurtzite character of the underlying heterocrystalline systems.

The central question, which has to be addressed, is whether the discussed heterocrystalline structures represent simply new polytypes with averaged properties or really "heterostructures" with completely new properties. For that purpose we study the resulting energy gaps as well as the localization of the band-edge wave functions in more detail. Rather astonishing is the magnitude of the indirect energy gaps $\Gamma_{6v} \rightarrow M_{1c}$ of 1.19 eV $[(3C)_2(6H)_2]$, 1.17 eV $[(3C)_2(4H)_3]$, 1.09 eV $[(3C)_2(2H)_6]$, or 0.75 eV $[(3C)_4(2H)_3]$ resulting within the DFT-LDA. They are in any case smaller than the smallest energy gap in a natural polytype, the zinc-blende $3C$-SiC, where the DFT-LDA value amounts to 1.27 eV. On the other hand, for all considered heterocrystalline combinations the character of a type-II heterostructure is expected [3,12]. The schematic band lineup of such a system is represented in Fig. 3 for the special case of $(3C)_{N_1}(2H)_{N_2}$. Because of the type-II character, a gap is expected which mainly arises from that of $3C$-SiC but is reduced by the valence-band discontinuity $|\Delta E_v|$. The calculated gaps follow this rule. However, the reduction is much larger than the valence-band offsets estimated for $3C/pH$ systems of 0.02 eV ($p = 6$), 0.05 eV ($p = 4$), and 0.13 eV ($p = 2$) [4,12], taking into account only the asymptotics of the pseudopotentials. That means that the valence-band portion of the total gap discontinuity is larger in real structures. This fact may be traced back to the influence of the self-consistency in the determination of electrostatic potential in the whole heterocrystalline structure. Its actual position changes the ratio of the conduction-band and valence-band discontinuities. The gap values under discussion are influenced by the quasiparticle effect; it opens the indirect energy gaps by somewhat more than 1 eV [4]. A principal change of the type-II character of the structures by quasiparticle effects seems to be excluded, since the maximum variation of the gap opening with the polytype is about 0.1 eV or even smaller.

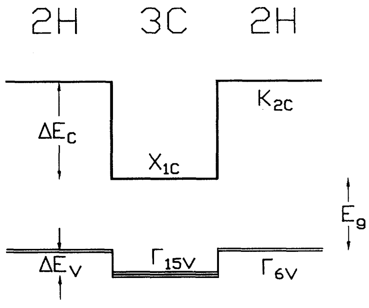

FIG. 3. Schematic representation of the band alignment for the lowest conduction-band states and the top of the valence band for a $(3C)_{N_1}(2H)_{N_2}$ heterocrystalline structure along the growth direction. Resulting gap and band offsets are also indicated.

The identification of the considered heterocrystalline combinations as type-II superlattices is supported by Fig. 4, where the localization of the Bloch wave functions for the lowest conduction band at K and M as well as the highest valence band at Γ is represented along the extent of a unit cell parallel to the c axis. The extreme combinations of the zinc-blende and wurtzite polytypes, $(3C)_2(2H)_6$ and $(3C)_4(2H)_3$, are represented. The figures clearly confirm the type-II character of the structure resulting for the $(3C)_4(2H)_3$ combination. The lowest conduction-band state at M is actually essentially localized in the $3C$ material with pure cubic stacking. The electrons are confined to the cubic part of the supercell. On the other hand, the highest valence state at Γ is localized in the hexagonally stacked $2H$-like region of the unit cell. Consequently, holes should appear in the hexagonal layers. The same localization is found for the K minimum of the conduction band. In contrast to our expectations, the corresponding electron wave function is mainly localized within the cubic bilayers. These findings may be explained in terms of the folding procedure and a repulsion of folded wurtzitelike bands. A further complication arises from the mentioned asymmetry of the two interfaces, which gives rise to the asymmetry in the probabilities to find the particles. We have to mention that after a increase of the hexagonal character of the heterocrystalline structure in the $(3C)_2(2H)_6$, the lowest conduction-band state is localized within $2H$-like layers as a consequence of the particle-in-the-box effect in the $3C$ material, which pushes the $3C$-like

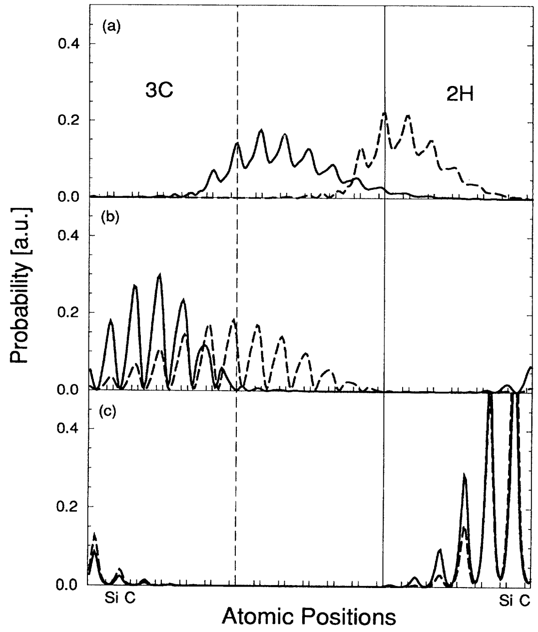

FIG. 4. Squared wave functions of lowest conduction-band states at M (a) and K (b) as well as of the highest valence band at Γ (c) for $(3C)_4(2H)_3$ (solid line) and $(3C)_2(2H)_6$ (dashed line) superlattices. In order to have an impression of the localization of electrons and holes, the probabilities are integrated over the plane perpendicular to the growth direction. The positions of Si and C atoms are indicated by vertical ticks. The vertical lines separate the $3C$ and $2H$ regions.

layers towards higher energies. Our test calculation for the $30H$ system, more strictly $(3C)_6(2H)_6$, shows that for thicker heterostructures the type-II character is again stabilized. However, the wave function of the conduction-band minimum at M is essentially localized near the interface $3C \longrightarrow 2H$.

In summary, we have found that the arrangement of different natural polytypes in heterocrystalline structures gives "heterostructurelike" materials with novel properties. The effect is explicitly shown for the combinations of cubic and hexagonal polytypes of SiC. We predict electronic properties of the heterocrystalline structures which correspond to those of a type-II heterostructure. The gap is not only indirect in the **k** space but also in the real space. The wave functions of the top of the valence band and of the bottom of the conduction band are localized in different space regions. Because of the present dramatic progress in the growth of SiC far from the equilibrium, we expect an experimental realization of the predicted heterocrystalline SiC structures made by different polytypes. Because of the resulting perfect interfaces without any alloying effect, interesting physical and technological applications are possible.

We are indebted to B. Wenzien for helpful discussions. This work was supported by the Sonderforschungsbereich 196 (project A08) of the Deutsche Forschungsgemeinschaft and the EC Programme Human Capital and Mobility under Contract No. ERBCHRXCT 930337.

[1] A.R. Verma and P. Krishna, *Polymorphism and Polytypism in Crystals* (Wiley, New York, 1966).
[2] *Numerical Data and Functional Relationships in Science and Technology,* edited by O. Madelung, Landolt-Börnstein New Series, Group III, Vol. 17a (Springer, Berlin, 1982); *ibid.,* Vol. 22a (Springer, Berlin, 1986).
[3] P. Käckell, B. Wenzien, and F. Bechstedt, Phys. Rev. B **50**, 10 761 (1994).
[4] B. Wenzien, P. Käckell, F. Bechstedt, and G. Cappellini, Phys. Rev. B (to be published).
[5] T. Sugii, T. Aoyama, and T. Ito, J. Electrochem. Soc. **137**, 989 (1990).
[6] H. Matsunami, Physica (Amsterdam) **185B**, 65 (1993).
[7] A. Fissel, B. Schröter, and W. Richter, Appl. Phys. Lett. **66**, 3182 (1995).
[8] W.J. Choyke, D.R. Hamilton, and L. Patrick, Phys. Rev. **133**, 1163 (1964).
[9] P. Käckell, B. Wenzien, and F. Bechstedt, Phys. Rev. B **50**, 17 037 (1994).
[10] C. Cheng, V. Heine, and R.J. Needs, J. Phys. Condens. Matter **2**, 5115 (1990).
[11] R. Stumpf and M. Scheffler, Comput. Phys. Commun. **79**, 447 (1994).
[12] A. Qteish, V. Heine, and R.J. Needs, Phys. Rev. B **45**, 6534 (1992).